

Mineralogical and Micromorphological Characterization of Iron Impurity in Gedikler Bentonite Mine (Esme/Usak, Turkey)

HATICE YILMAZ* and UGUR KÖKTÜRK

Department of Mining Engineering, Dokuz Eylul University,
Tinaztepe Campus, 35160 Buca, Izmir, Turkey
E-mail: hatice.yilmaz@deu.edu.tr

This paper deals with the determination of iron impurity in samples collected from the Gedikler (Esme) bentonite mine in Usak area, Turkey. Although the chemical analysis of the samples shows that their iron contents vary from 1.93 to 4.04 Fe₂O₃ %, any iron mineral could not be determined by X-ray diffraction (XRD) analysis in the raw samples. Hence, magnetic separation process was applied to the samples. XRD analysis followed by magnetic separation indicated that the major mineral of magnetic product (MP) is jarosite and there are minor amounts of smectite, kaolinite and opal-CT. In addition to XRD analysis of magnetic product, chemical analysis showed that it mainly consists of Fe₂O₃, K₂O, SO₄²⁻ and high LOI. In addition to confirm this deduction, the molecular equivalents of these elements, which were calculated based on these results, imply the presence of jarosite. These results were also supported by simultaneous thermo gravimetric/differential thermal analysis (TG/DTA) and infrared spectroscopy (IR) studies. Scanning electron microscopy (SEM) combined with energy-dispersive spectroscopy (EDS) analysis revealed that the magnetic product predominantly consists of pseudo cubic crystals in which mainly Fe, K, S, O and minor amount of Al is present. The presence of Al in crystals shows that some of the Fe positions are probably filled with Al. Based on these data, it is concluded that the iron mineral of the Gedikler bentonite mine is jarosite-alunite solid solution and it can be eliminated by magnetic separation easily.

Key Words: Magnetic separation, XRD, IR, DTA-TGA, SEM-EDS, Jarosite.

INTRODUCTION

Bentonites are used extensively in the production of food, pharmaceuticals, cosmetics, animal feeds, fertilizers, catalyzer and pesticides. The uses of bentonites in various processes are closely related to their structure, chemical and mineralogical composition¹. The bentonites consist mainly of different smectite group minerals, non-clay minerals and trace amount of organic materials^{2,3}. While the major smectite group minerals are montmorillonite, nontronite, saponite, beidellite and hectorite, the most common non-clay minerals in bentonites are feldspars, zeolites, carbonates, gypsum, pyrite, silica polymorphs, iron oxides and iron sulfate minerals⁴⁻⁶. Although non-clay mineral contaminations in most cases are very low, they can significantly

affect the properties of bentonite. For example, while the presence of amorphous silica increases the plasticity of the bentonite⁷, silica polymorphs such as opal-CT, cristobalite, quartz, *etc.*, give abrasive properties to the bentonites⁸. Similarly, iron oxides colour bentonite red and, hence, it is not desirable to use such bentonite in most sectors such as oil bleaching and catalysis. Therefore, it is necessary to determine and remove the iron bearing impurities. Normally, these minerals can be identified by their characteristic X-ray diffraction patterns. However, if the concentrations of minerals are too low, it is difficult to obtain sufficient number of diagnostic reflections in the XRD patterns. In this case, it can be useful to concentrate these minerals using appropriate methods. It is well known that all the iron minerals have high magnetic susceptibilities and they can be extracted from the other minerals with low magnetic susceptibility by magnetic separation.

In Gedikler bentonite samples, smectite is the main clay mineral; kaolinite, opal-CT, K-feldspar and quartz complete the mineralogical suite⁹. Although the samples contain 1.93-4.04 Fe₂O₃ %, any iron bearing mineral could not be detected by XRD analysis. If the iron bearing impurities determine and remove from bentonite, this bentonite can be used in oil bleaching sector. The aim of this study is to determine the iron bearing impurities and to remove them with a suitable method. Hence, magnetic separation method combined with analytical methods (XRD, DTA/TG, IR, SEM-EDS, chemical analysis and heating process) was used to facilitate the identification of the iron mineral/or minerals which cause the iron impurity and to remove them.

EXPERIMENTAL

Materials and sample preparation: Four samples were taken from the Gedikler bentonite mine. Air dried samples were crushed with a jaw crusher to pass through a 5 mm sieve and then the crushed samples were ground with an automatic agate mortar to pass through a 0.053 mm sieve. Ground samples were dried at 105 °C for 24 h and then were cooled for 10-15 min in a pyrex desiccator to prevent hydration. These samples were used for mineralogical characterization. But, in this study the characterization was focused on the sample 3 which has the highest iron content since all the samples have the same mineralogical composition. From here onwards, sample 3 is called as raw bentonite.

It is known that iron minerals have extremely high mass absorption coefficients when Cu radiation is used in XRD studies. Because CuK_α radiation is strongly absorbed by iron minerals and a high background is produced due to the fluorescence radiation¹⁰. Accordingly, it is not easy to determine iron minerals at low concentration by XRD when CuK_α radiation is used. In such situations, it is necessary to concentrate the iron minerals. Many iron minerals except magnetite which is a natural mineral having the highest magnetic susceptibility, have generally medium level magnetic susceptibility and can be easily separated with high intensity magnetic separator from the other minerals¹¹. Fig. 1 shows the block diagram used in the beneficiation and characterization of raw bentonite.

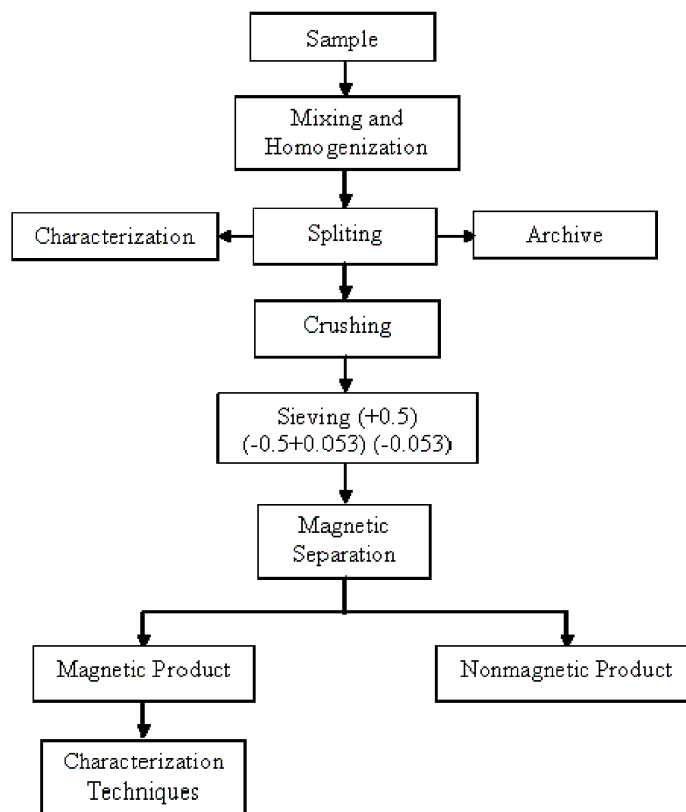


Fig. 1. Block diagram used in the beneficiation and characterization studies of iron bearing mineral from the Gedikler (Esme/Usak, Turkey) bentonite mine

According to this diagram, the raw bentonite was crushed below 5 mm and was divided into + 0.5 mm, (-0.5+0.053) mm, (-0.053) mm fractions by wet sieving. The sieve fractions were dried at 105 °C for 24 h. Each of these fractions was fed to high intensity dry magnetic separator (Type: L/P10-30, International Process Systems Inc.) at 1.8 T magnetic field intensity to obtain magnetic and nonmagnetic products. While raw bentonite has generally yellowish cream colour and in patches yellowish brown colour, nonmagnetic product (NP) has mainly yellowish cream colour and magnetic product (MP) has mostly yellowish brown colour. Then, in order to identify the iron impurity in the Gedikler bentonite mine was studied on the magnetic product.

Analytical methods: The mineralogical composition of the samples was determined by powder XRD analysis technique. The XRD patterns of the samples were recorded from randomly oriented amounts by using a Jeol JSDX-100S4 powder diffractometer, operating at 32 kV and 22 mA, using Ni-filtered $\text{CuK}\alpha$ X-ray, having 1.54 Å wavelength, at a scanning speed of 2° 2θ/min and chart speed of 20 mm/min.

Major element analysis of the raw bentonite and magnetic product which were prepared using the $\text{Li}_2\text{B}_4\text{O}_7$ fusion method¹² was carried out with Varian atomic

absorption spectrometer. Loss on ignition (LOI), *i.e.* the content of water and other volatiles in wt. %) was determined at 1000 °C for 1 h on the dried samples. Sulphate analysis was performed by gravimetric method.

Thermal behaviour of magnetic product was investigated with a Linseis DTA-TG, L-81 instrument by heating about 70 mg of the specimen in the temperature range 20-1000 °C (at a heating rate of 10 °C/min) using α -Al₂O₃ as a reference material in air atmosphere. In addition, magnetic product was heated at 1000 °C for 1 h in order to determine the heat stability of the iron-bearing mineral. After cooling to room temperature in a pyrex desiccator, the residues of this heat treatment labeled as heated magnetic product (HMP) were stored for characterization.

The infrared spectrums of raw bentonite and magnetic product were obtained by Shimadzu IR 470 spectrometer. 2 mg of each sample previously dried at 105 °C were mixed with 200 mg KBr homogeneously and pressed on disks.

The micro morphological features and semi-quantitative element analysis of the magnetic product were examined with Jeol-6060A SEM, equipped with EDS. Sample particles ~ 5 mm in size were cemented with carbon band on to brass stubs and coated with gold-palladium. The SEM and EDS studies were carried out using an accelerating voltage of 20 kV.

RESULTS AND DISCUSSION

Mineralogical and chemical characterization: The mineralogical composition of the raw bentonite, as determined by XRD analysis, is given in Fig. 2. According to this figure, raw bentonite consists mainly of smectite, kaolinite, opal-CT and minor amounts of quartz, K-feldspar. However, there is a weak peak of 3.08 Å is not attributable to aforementioned minerals. In order to determine the source of this peak, chemical analysis was applied to the raw bentonite.

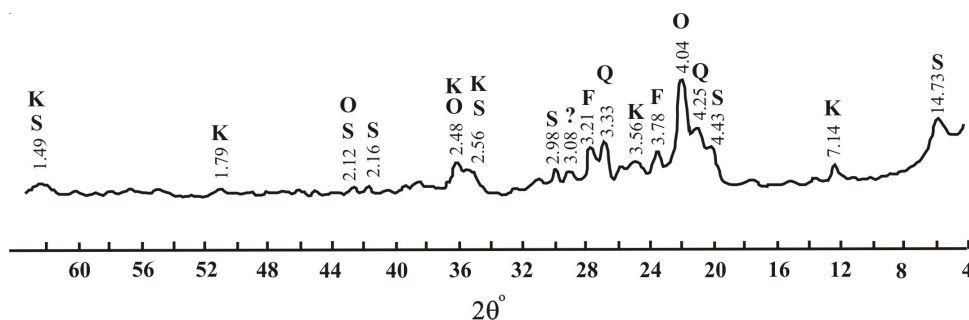


Fig. 2. XRD pattern of the raw bentonite. S: smectite, K: kaolinite, O: opal-CT, F: K-feldspar, Q: quartz, ? : unknown mineral

Table-1 shows the chemical composition of the raw bentonite. According to these results Al₂O₃, SiO₂, Fe₂O₃ and LOI values are very high, while alkali oxides (Ca, Mg and Na) are present only in very small amounts, except K₂O. These results reflect the chemical composition of the raw bentonite. Although, high Fe₂O₃ was

detected in the chemical analysis of the bentonite samples, any iron-bearing minerals did not determined by XRD analysis. Moreover, exchangeable cation analysis showed that iron is not exchangeable cation in bentonite sample⁹. In this case, the peak of 3.08 Å can be an iron mineral due to the Fe₂O₃ (4.04 %) content of the raw bentonite (Table-1), yet the low intensity of this peak makes the mineralogical identification difficult. For this reason, magnetic separation (Fig. 1) was applied to the raw bentonite in order to concentrate the probable iron minerals. Magnetic product obtained from magnetic separation was used to characterize the iron mineral/ or minerals which cause the iron impurity.

TABLE-1
CHEMICAL COMPOSITION OF THE RAW BENTONITE (wt. %)

Oxides	Weight (%)	Oxides	Weight (%)
SiO ₂	58.05	MgO	0.28
Al ₂ O ₃	20.82	Na ₂ O	0.03
Fe ₂ O ₃	4.040	K ₂ O	0.89
CaO	0.110	Loss on ignition (LOI)	15.12

The XRD diagram of the magnetic product is also seen in Fig. 3. This diagram is notably different from raw bentonite's (Fig. 2). It has also shown that the intensity of reflection of 3.08 Å in which the XRD pattern of the raw bentonite increased and also new peaks appeared. Because of that, the diagnostic reflections of smectite, opal-CT and kaolinite could hardly be identified in the XRD pattern of the magnetic product. While almost all these diagnostic XRD reflections seen in Fig. 3 can be attributable to jarosite [KFe₃(SO₄)₂(OH)₆]¹³, the low intensity reflections of 14.2, 3.59 and 4.04 Å belong to smectite, kaolinite and opal-CT respectively. The low intensity of the XRD peaks of these minerals can be explained by their low concentration in the magnetic product.

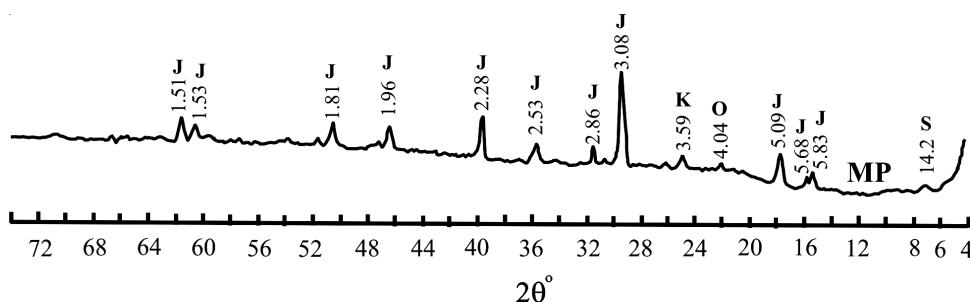


Fig. 3. XRD pattern of magnetic product. S: smectite, K: kaolinite, O: opal-CT, J: jarosite

These results are also coherent with the chemical analysis of the magnetic product (Table-2). Because raw bentonite is composed of mainly smectite, kaolinite

and opal-CT, and minor amounts of K-feldspar, quartz and jarosite (Fig. 2), it shows high SiO₂, Al₂O₃ and LOI values (Table-1). Magnetic product consists of mainly jarosite and less amounts of smectite, kaolinite and opal-CT (Fig. 3) and therefore, has extremely high K₂O, Fe₂O₃, SO₄²⁻ and LOI values (Table-2). Both the raw bentonite and magnetic product have high LOI values, but the magnetic product has a higher LOI value compared to raw bentonite. Since smectite absorbs water, high LOI value of raw bentonite is an indication of smectite. But high LOI value of the magnetic product results largely from jarosite because one mole jarosite contains 2 mol SO₃ and 3 mol H₂O.

TABLE-2
CHEMICAL COMPOSITION OF THE MAGNETIC PRODUCT (wt. %)

Oxides	Weight (%)	Oxides	Weight (%)
SiO ₂	11.370	Na ₂ O	0.06
Al ₂ O ₃	9.130	K ₂ O	7.27
Fe ₂ O ₃	34.710	Loss on ignition (LOI)	37.22
CaO	0.081	SO ₄ ²⁻	28.36
MgO	0.036	—	—

In order to be able to calculate the molecular equivalent of the components of jarosite in magnetic product, it was assumed that the entire sulfate in Table-2 is originated from jarosite. Thus the molecular equivalents of the alkalis were based on a figure of 4.00 for the molecular equivalent of SO₃. The molecular equivalent of K₂O and Fe₂O₃ were calculated as 1.04 and 2.94, respectively, which can be accepted as 1 and 3 approximately (Table-3). In addition, if the presence of the K-feldspar in the sample is considered, it will not be surprising that the molecular equivalent of K₂O is 1.04. In the magnetic product, there is deficiency in the molecular equivalent of the Fe₂O₃ and this deficiency can be completed by substitutions aluminum in the iron positions. Because jarosite is an alunite family mineral whose general composition¹⁴ is AB₂(SO₄)₂(OH)₆. In which A may be K⁺, Na⁺, Pb²⁺, HN₄⁺ or Ag⁺ and B either Fe³⁺ or Al³⁺.

TABLE-3
MOLECULAR EQUIVALENTS OF THEORETICAL JAROSITE AND
MAGNETIC PRODUCT IN RELATION WITH THEIR CHEMICAL COMPOSITION

Sample	Oxides	Wt %	Molecular equivalents
Theoretical jarosite	K ₂ O	9.38	1.00
	Fe ₂ O ₃	47.90	3.00
	SO ₃	31.94	4.00
Magnetic product	K ₂ O	7.27	0.077=1.04
	Fe ₂ O ₃	34.71	0.217=2.94
	SO ₃	23.63	0.295=4.00

Infrared spectra of the raw bentonite and magnetic product are presented in Fig. 4. The magnetic product and raw bentonite have similar infrared spectrums despite their different bands. The raw bentonite spectrum consists predominantly of smectite that belongs to 3630, 3420, 1635, 1035, 522 and 467 cm^{-1} bands, kaolinite that belongs to 3635, 1031, 935 cm^{-1} bands, opal-CT that has 1100 and 785 cm^{-1} bands and only one jarosite distinctive IR absorbance band of 3360 cm^{-1} , while the magnetic product spectrum results mainly from jarosite and minor smectite, kaolinite and opal-CT bands.

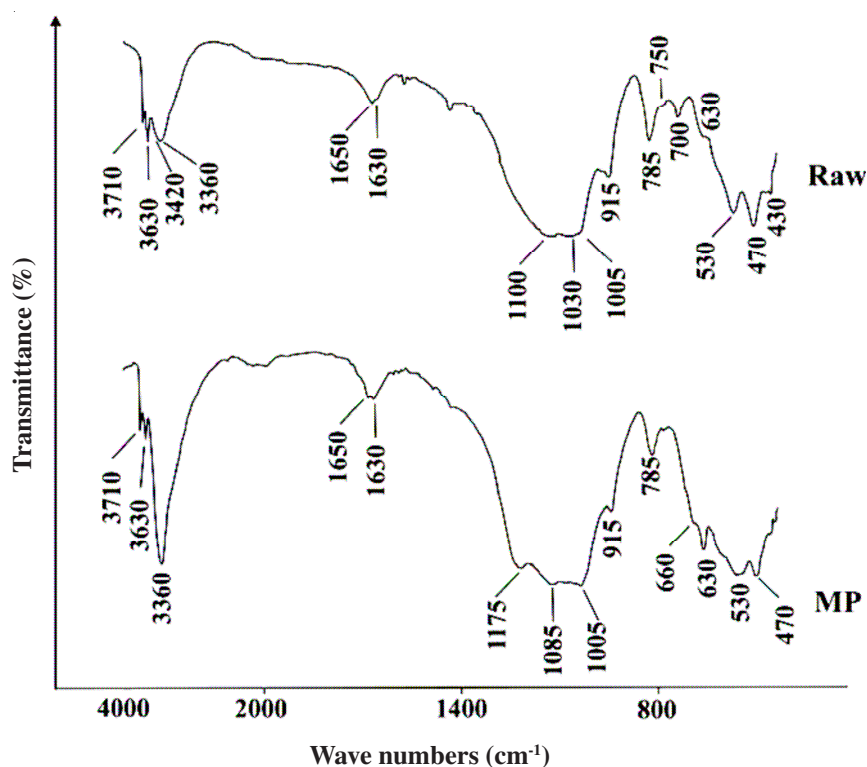


Fig. 4. Infrared spectrums of raw bentonite and magnetic product (MP)

In infrared spectra of magnetic product, the distinctive IR absorbance frequencies of jarosite dominate while there are only very weak two absorption bands of smectite and kaolinite near 3630, 1630 cm^{-1} and 3630, 915 cm^{-1} , respectively. The distinctive IR bands in the spectrum at 1200-1190 and 1090-1080 cm^{-1} (ν_3 mode of SO_4^{2-}), at 1030-1010 cm^{-1} (ν_1 mode of SO_4^{2-}), at 650-640 cm^{-1} (ν_4 mode of SO_4^{2-}), at 3400-3300 cm^{-1} (stretching mode of OH), at 1010-1000 cm^{-1} (σ mode of OH) and at 480-470 cm^{-1} (τ mode of OH) relate to jarosite^{15,16}. In this spectrum, the stretching band of OH at 3400-3300 cm^{-1} is the most decisive one due to the increasing intensity.

Thermal characterization of magnetic product: After iron mineral in magnetic product was identified as jarosite, differential thermal (DTA/TG) analysis was carried out on it (Fig. 5). In DTA curve, the exotherm at 498.8 °C can be explained as the crystallization of α -Fe₂O₃. Endotherm at range 360-480 °C (peak position at 439.3 °C) represents dehydration and the second endotherm at 767.9 °C stands for the decomposition of the double sulfate formed on dehydration¹⁷. Additionally, weight losses of 8.7 and 14.32 % accompany to the first and second endotherms, respectively. These results agree with the DTA-TG curves of jarosite given by McLaughlin¹⁷ and the data obtained from heating process. But the peak temperatures found in this study differ from those of McLaughlin, probably because of their faster heating rate (12.5 °C instead of 10 °C/min)¹⁸ and the impurity of the magnetic product concentrated using magnetic separation.

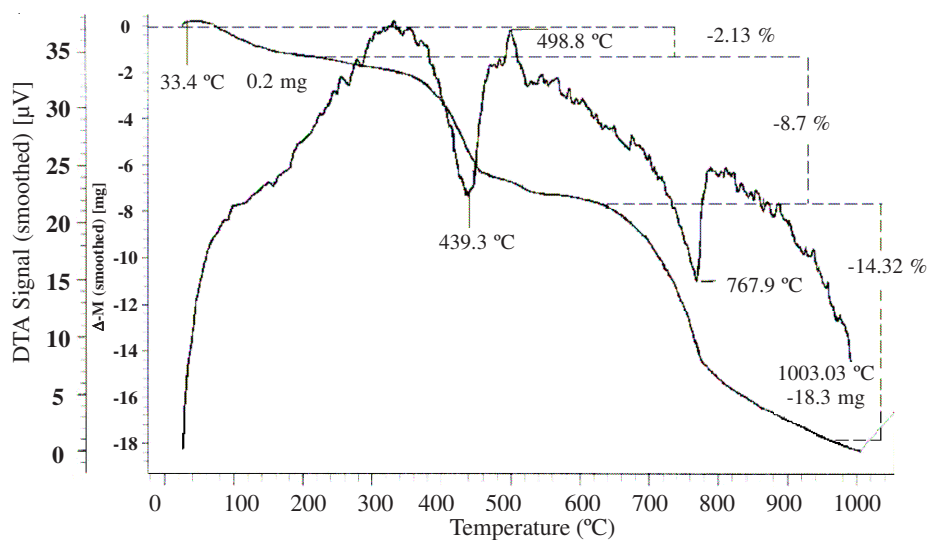


Fig. 5. DTA-TG diagrams of the magnetic product range from 22-1000 °C

Warshaw¹⁸ stated that the X-ray patterns remain unchanged up to the start of the first endothermic reaction, during which the colour changes from yellowish brown to brown and the XRD lines of the sulfate mineral disappear. After the material heated for a longer time or at a higher temperature, it takes on a reddish brown colour and changes into hematite. This situation which is the change of colour from yellowish brown to reddish brown was also observed while the LOI values of magnetic product was analyzed at 1000 °C. This change showed that jarosite is an unstable mineral at high temperatures. So, in order to determine the stable mineral which is formed when jarosite was heated to 1000 °C, residue (heated magnetic product, HMP) is X-rayed. It was found that all diagnostic jarosite and kaolinite reflections disappeared and almost all characteristic hematite (α -Fe₂O₃) reflections and only one α -hyperoxide potassium (α -KO₂) reflection of 3.34 Å came out due to high

mass absorption coefficient for $\text{CuK}\alpha$ radiation as being iron oxides (Fig. 6). However, the most characteristic reflection for opal-CT of 4.04 \AA stayed still in place after the heat treatment whereas the smectite reflection of 14.73 \AA collapsed to 9.6 \AA and its intensity decreased. These results are in harmony with the literature^{4,19-22}. After heating to $500 \text{ }^\circ\text{C}$, while the decaying of the kaolinite reflection can be explained by the changing amorphous phase, the disappearance of the smectite reflection of 14.73 \AA can be explained by the destruction of its crystal structure where this reflection collapses to 9.6 \AA and its intensity decreases^{4,20}. Also jarosite changes into hematite completely in a short time when it is heated to over $500 \text{ }^\circ\text{C}$ ¹⁷. Normally opal-CT changes into α -cristobalite when its temperature is over $1050 \text{ }^\circ\text{C}$ for 24 h ^{21,22} but this transformation did not take place in this study because of the insufficient treatment time. These results also explain the transformation of yellowish brown jarosite to hematite with a reddish brown colour.

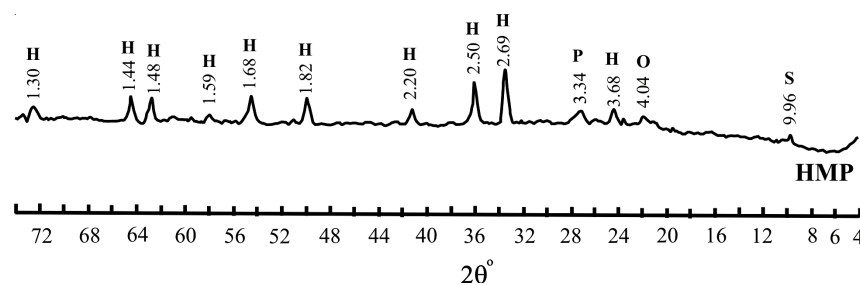


Fig. 6. XRD patterns of the HMP (heated magnetic product). S: Smectite, O: opal-CT, H: hematite, P: α -hyperoksite potassium)

Micromorphology and EDS analysis of magnetic product: SEM observations also proved that the magnetic product sample is composed primarily of aggregates pseudocubic crystals in the range of $0.1\text{-}0.7 \mu\text{m}$ (Fig. 7). According to the results of XRD, IR and DTA-TG studies, chemical analysis and heating process of magnetic product, these crystals must be jarosite. Normally, jarosite has the hexagonal crystal structure although Sasaki and Konno¹⁶ obtained mostly of round and granular particles, and undeveloped sharp edges. But, Herbert¹⁰ expressed that jarosite from a mine drainage environment using chemical extraction techniques, precipitated as pseudocubic crystals is similar to the samples of this study. Similarly, Akai *et al.*²³ reported that the shape of crystals of natural jarosite at the Gunma iron mine, Japan, which is abiogenic in origin and pseudocubic. The differences in the crystal shapes in these studies may stem from the crystallization conditions. Moreover, the EDS analyses revealed that the pseudocubic crystals in the magnetic product (Fig. 7) consisted mainly of K, Fe, S and O and minor amounts of Al. The presence of Al at these crystals is noteworthy due to the supporting equivalent molecular calculations (Table-3). The deficiency of iron could be determined not only in molecular equivalent calculations but also in the EDS analysis. So, the SEM-EDS analyses show that these crystals are jarosite more precisely jarosite-alunite solid solution, indicating, stoichiometric molar composition both macro and micro scale.

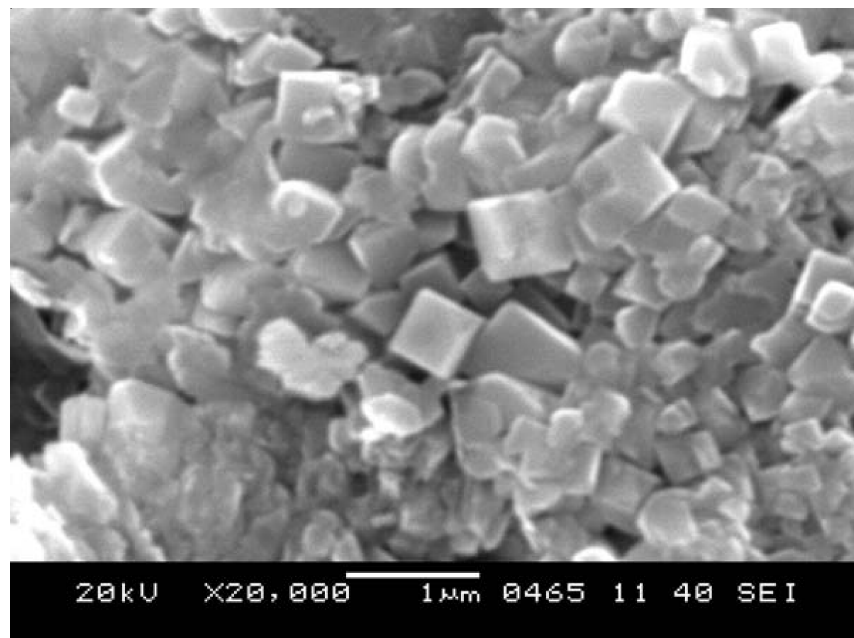


Fig. 7. SEM images of well formed pseudocubic jarosite crystals displaying casts of step growth features

Conclusion

Bentonite samples were collected from the Gedikler (Esme) bentonite mine in Usak area of Turkey and enriched by magnetic separation process to determine iron impurities of the bentonite samples. The magnetic product derived from magnetic separation was assessed by XRD analysis for identification of the iron mineral or minerals. XRD analysis show that jarosite accompanied by smectite, kaolinite and opal-CT are the main products of the magnetic product. The presence of jarosite is also confirmed using molecular equivalent calculation. In addition, the assessment of magnetic product was made using various methods, such as simultaneous thermo gravimetric/differential thermal analysis and infrared spectroscopy. Identification of the pseudo cubic jarosite is based on SEM analysis supported by the EDS analysis showing the major elements of jarosite (K, Fe, S, and O with additional minor amount of Al). The presence of Al in jarosite structure can be attributed to jarosite-alunite solid solution. Based on the available data, it is deduced that the iron impurity of Gedikler (Esme) bentonite mine is jarosite-alunite solid solution and it can be removed by magnetic separation method.

ACKNOWLEDGEMENT

This study was supported by Scientific Research Project Division of Dokuz Eylul University, Turkey (Project Number: 02.KB.FEN.050).

REFERENCES

1. S. Kaufhold, R. Dohrmann, K. Ufer and F.M. Meyer, *Appl. Clay Sci.*, **22**, 145 (2002).
2. R.E. Grim, *Clay Mineralogy*, McGraw-Hill Book Company, New York, edn. 2 (1968).
3. R.E. Grim, *Clays & Clay Minerals*, **36**, 907 (1988).
4. D.M. Moore and R.C. Reynolds Jr., *X-Ray Diffraction and Identification and Analysis of Clay Minerals*, Oxford University Press, Oxford (1989).
5. G.E. Christidis, *Clays & Clay Minerals*, **46**, 379 (1998).
6. H. Yalcin and G. Gumuser, *Clay Minerals*, **35**, 807 (2000).
7. <http://www.nishikigoi-info.com/koi-care/koi-clay.html>
8. G.E. Christidis and P.W. Scott, *Mineralium Deposita*, **32**, 271 (1997).
9. H. Yilmaz, X-ray Diffraction Method in the Determination of the Enrichment Ratio of Clay Minerals and Their Industrial Applications, Ph.D. Thesis, Dokuz Eylul University, The Graduate School of Natural and Applied Sciences, Turkey (2004) (in Turkish).
10. R.B. Herbert, *Clays & Clay Minerals*, **45**, 261 (1997).
11. S. Rosenblum and I.K. Brownfield, Magnetic Susceptibilities of Minerals, S.S. Geological Survey, U.S. Department of the Interior Open File Report, 99-529 (1999).
12. Perkin-Elmer, Analytical Methods for Atomic Absorption Spectrophotometry, Perkin-Elmer Corporation, USA (1976).
13. JCPDS, Powder Diffraction File, Joint Committee on Powder Diffraction Standards 1601 Park Lane, Swarthmore, Pennsylvania 19081 (1972).
14. G.P. Brophy, E.S. Scott and S.A. Snellgrove, *Am. Mineral.*, **47**, 112 (1962).
15. R.J.P. Lyon, in ed.: J. Zussman, Infrared Absorption Spectroscopy, Physical Methods in Determinative Mineralogy, Academic Press, London and New York, pp. 371-404 (1967).
16. K. Sasaki and H. Konno, *Can. Mineralog.*, **38**, 45 (2000).
17. R.J.W. McLaughlin, in ed.: J. Zussman, Thermal Techniques, Physical Methods in Determinative Mineralogy, Academic Press, London and New York, pp. 405-444 (1967).
18. C.M. Warshaw, *Am. Mineralog.*, **41**, 288 (1956).
19. H.P. Klug and L.E. Alexander, *X-Ray Diffraction Procedures for Polycrystalline and Amorphous Materials*, Wiley-Interscience Publication, John Wiley & Sons, New York (1974).
20. W. Stumm and J.J. Morgan, *Aquatic Chemistry, An Introduction Emphasizing Chemical Equilibria in Natural Waters*, Wiley-Interscience Publication John Wiley & Sons, New York (1981).
21. S. Kahraman, M. Onal, Y. Sarikaya and I. Bozdogan, *Anal. Chim. Acta*, **552**, 201 (2005).
22. M. Onal, S. Kahraman and Y. Sarikaya, *Appl. Clay Sci.*, **35**, 25 (2007).
23. J. Akai, K. Akai, M. Ito, S. Nakano, Y. Maki and I. Sasagawa, *Am. Mineral.*, **84**, 171 (1999).